Optical Engineering

SPIEDigitalLibrary.org/oe

Micro-hole drilling and cutting using femtosecond fiber laser

Huan Huang
Lih-Mei Yang
Jian Liu

SPIE

Micro-hole drilling and cutting using femtosecond fiber laser

Huan Huang,* Lih-Mei Yang, and Jian Liu
PolarOnyx, Inc., 2526 Qume Drive, Suite 17 & 18, San Jose, California 95131

Abstract. Micro-hole drilling and cutting in ambient air are presented by using a femtosecond fiber laser. At first, the micro-hole drilling was investigated in both transparent (glasses) and nontransparent (metals and tissues) materials. The shape and morphology of the holes were characterized and evaluated with optical and scanning electron microscopy. Debris-free micro-holes with good roundness and no thermal damage were demonstrated with the aspect ratio of 8:1. Micro-hole drilling in hard and soft tissues with no crack or collateral thermal damage is also demonstrated. Then, trench micromachining and cutting were studied for different materials and the effect of the laser parameters on the trench properties was investigated. Straight and clean trench edges were obtained with no thermal damage. [DOI: 10.1117/1.OE.53.5.051513]

Keywords: femtosecond laser; fiber laser; drilling; micro-hole; cutting; micromachining.

Paper 131230SS received Aug. 13, 2013; revised manuscript received Dec. 19, 2013; accepted for publication Jan. 10, 2014; published online Feb. 13, 2014.

1 Introduction

Laser micromachining has received much attention due to the broad applications across nearly all manufacturing sectors. Among the major applications, laser micro-hole drilling and cutting are widely used in aeronautic, automobile, semiconductor, and biomedical industries such as aircraft engine turbine blades, automotive fuel filters, combustion chambers, surgical needles, and microfluidic devices. The demand for high-aspect-ratio micro-holes in different materials (both transparent and nontransparent) is increasing in micro-pumps, micro-sensors, micro-chemical-reactors, and micro-heat-exchangers to obtain higher efficiency and performance. For micro-hole drilling, the current fabrication method still heavily relies on photolithography techniques, which require advanced facilities and numerous process steps. They are often limited in material type and geometry. Drilling and cutting with nanosecond (ns) or longer pulsed laser are always accompanied with the formation of melting and recast layer. Although the geometrical precision could be improved by using techniques such as helical drilling or wobbling, the quality and precision achievable with ns laser pulses are still limited due to the uncontrolled redeposition of the melt. Drilling and cutting with picosecond (ps) pulsed laser still have detrimental effects such as cracks and heat-affected zone in the surrounding area due to the high energy input and thermally induced stress. This affects not only the accuracy but also the reliability of the process.

Recently, the development of femtosecond (fs) laser sources has provided a precise and versatile method for micro-scale and even nano-scale fabrication techniques. The physics behind the fs laser process is that pulses are ultrashort so that only material ablation by nonlinear absorption takes place, where longer pulsed or CW lasers introduce thermal heat deforming cutting edges and inducing cracks and stress. The main advantages of fs laser drilling and cutting lie in the low heat input and the reduction of melt component.

Many researchers have paid much attention to the micro-hole drilling and micro-cutting using fs lasers, including both transparent materials[1–9] and nontransparent materials.[10–15] Especially for transparent materials, different methods have been used to generate high-aspect-ratio micro-holes such as combination with chemical etching,[4,5] beam shaping,[2,6] and liquid-assisted drilling from rear surface.[1,3,7] However, the fs laser sources, generally, are traditional solid-state lasers, which are expensive, bulky, and need regular maintenance. This disadvantage can be overcome by fs fiber laser, which is much cheaper, more compact, reliable, and maintenance-free. Although there exist abundant studies on micro-hole drilling by fs lasers, drilling high-aspect-ratio micro-holes with minimal or no thermal damage still remains a major challenge.

In this paper, micro-hole drilling and cutting using a fs fiber laser (1030 nm wavelength and 750-fs pulse duration) were investigated. Examples of micro-hole drilling and cutting are included with discussions on their potential applications. Debris-free micro-holes with good roundness and no thermal damage were demonstrated for different materials. Furthermore, no crack or collateral thermal damage is observed for both hard and soft tissue drillings. Then trench micromachining and cutting were also studied for different materials and the effect of the laser parameters on the trench properties was investigated.

2 Methods and Materials

Figure 1 shows the sketch of the work station used in this study for laser micro-holes drilling and cutting. The fs laser system is a commercial mode-locked fiber laser (Uranus Series, PolarOnyx Laser Inc., San Jose, California), generating 750-fs pulses (FWHM) at 1030 nm wavelength with pulse repetition rate tunable from 1 Hz up to 1 MHz. The output collimated beam is a nearly symmetric Gaussian with $M^2 < 1.3$, and the maximum output pulse energy is

*Address all correspondence to: Huan Huang, E-mail: hhuang@polaronyx.com

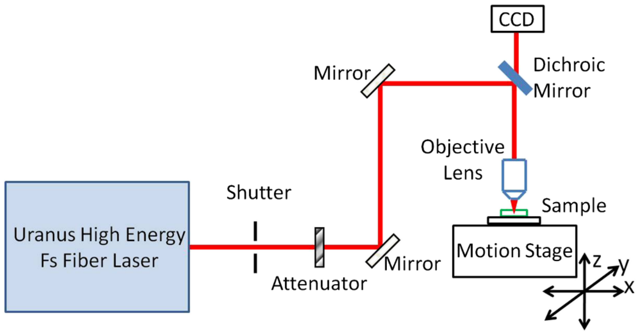

Fig. 1 Experimental setup for fs laser micromachining using microscope objective.

500 μJ. The laser beam is linearly polarized and two different micromachining conditions were used—microscope objective lens with motion stage and two-dimensional (2-D) scanner with F-theta lens. The focal spot diameters for the laser beam can be calculated by the diffraction limit, and the focal spot diameters for microscope and scanner methods are about 5 and 25 μm, respectively. The total loss of the beam delivery system is <50%. Such a loss has been accounted for in the irradiation pulse energy values stated hereafter. The laser pulse energy and repetition rate can be controlled via an acousto-optic modulator (AOM), and a mechanical shutter is used to switch the laser beam. A CCD camera is placed along the optical axis and used to align the sample and obtain a live view for the laser processing.

Simple percussion drilling cannot fulfill the requirements of high precision and quality. Trepanning drilling was used in this study. All experiments were performed in ambient air and without shielding gas, except for a transverse air flow to remove the ablation debris and shielding particles. The linear motion stage and the delay generator for AOM are controlled by computer to achieve different sample moving speeds and different pulse repetition rates.

In this study, different materials were used, including metals (stainless steel and titanium), glass (soda lime glass) and tissues (bovine bone and tendon). The bulk of these materials were cleaned before each experiment by isopropanol. Both metal and glass samples used were in the form of rectangular plates. The tissue samples were cut and prepared from fresh bovine bone and tendon from the local supermarket.

After the laser micromachining, the micro-topography of the drilled holes and cut features was characterized with an upright digital microscope (ME520T). Then the detailed quality was checked and measured by a scanning electron microscopy (SEM, FEI QUANTA FEG 600).

3 Results and Discussion

Traditional thermal processing uses long-pulsed or continuous-wave (CW) lasers and it works only for selected materials that absorb at the laser wavelength. In contrast, the high peak intensity generated by fs laser in the focal region can ionize a wide range of materials and creates hot plasma at the interface without impacting surrounding area (i.e., heat-affected zone free). As the molten pool is localized and quickly built up only in the vicinity of the focus, the thermal stress and thermally induced cracks are largely suppressed. The high intensity inside the focal volume will induce multiphoton or tunneling ionization and subsequent avalanche ionization. Substantial plasma generation and absorption enable the ablation of materials that are normally difficult to ablate by conventional lasers, such as transparent or low-absorption materials. This gives the unique capability of transparent material processing using fs laser.

At the beginning, the ablation thresholds for different materials were determined, which refer to the minimal energy density required to initiate material removal. Laser ablation just above the ablation threshold is called "gentle" and it usually allows a precise and clean material removal. A well-known method for the evaluation of the ablation threshold is used when the Gaussian beam was applied. Craters were made on the surface of the samples. Their diameters were measured and plotted versus laser pulse energy used to ablate the crater. The threshold was estimated from the relationship between the laser fluence and the diameter D of a crater created with a pulse.

For laser pulses with a Gaussian spatial beam profile, the maximum irradiation fluence F_0 can be calculated from the irradiation pulse energy E and the beam focus radius r as

$$F_0 = 2E/\pi r^2. \tag{1}$$

If the maximum fluence F_0 exceeds the ablation threshold fluence F_{th}, the squared diameter D^2 of the ablation crater is correlated as[16]

$$D^2 = 2r^2 \ln(F_0/F_{\mathrm{th}}). \tag{2}$$

As shown in Fig. 2, the single-shot ablation test of typical materials (dielectric, semiconductor, and metal) is investigated and the squared diameter of the ablated areas is plotted as a function of the laser fluence. The extrapolation to zero of the linear fit yields the single-shot ablation threshold. The ablation threshold for these materials is calculated as 2.70, 2.39, and 1.20 J/cm^2, respectively, for soda lime glass, silicon, and aluminum. The ablation threshold is expected to decrease for an increasing number of overlapping pulses due to material-dependent "incubation effect." Multishot ablation threshold can be determined by analyzing the diameter of ablation craters generated with multiple laser pulses, and it is not the focus of this study.

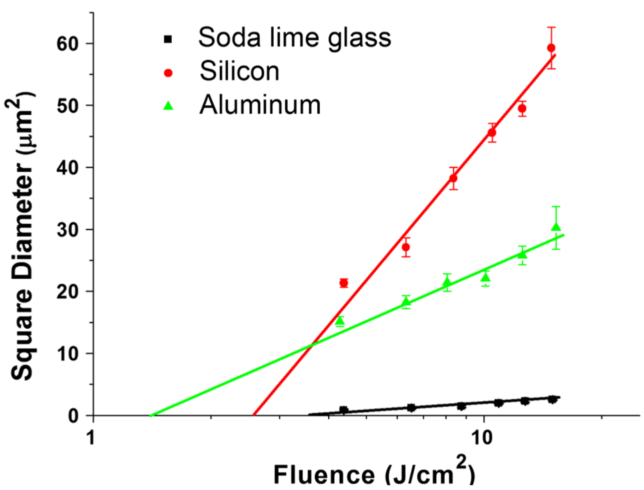

Fig. 2 Single-shot ablation threshold measurement for different materials by using fs laser.

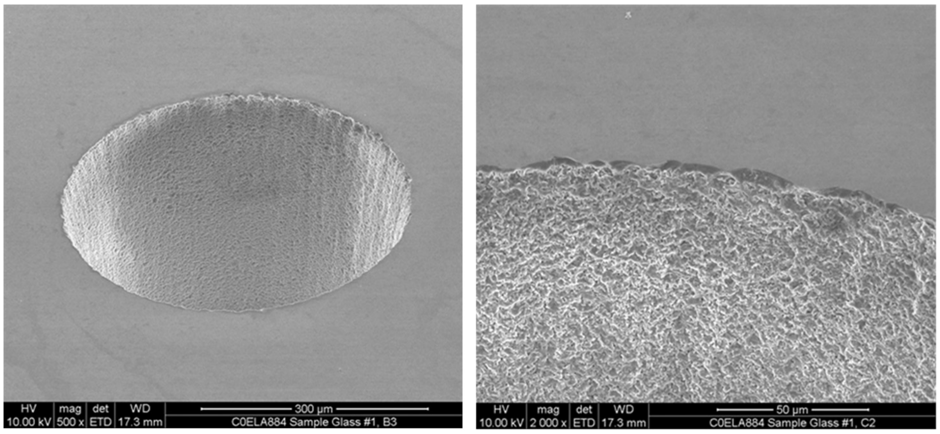

(a) (b)

Fig. 3 Scanning electron microscope (SEM) view of the drilled hole in soda lime glass using fs fiber laser: (a) Overview and (b) detail view of the hole edge and sidewall.

Then successive drilling was performed in different materials. Here, trepanning drilling technique was used since it can generate relative large holes with good consistency and hole taper compared with percussion drilling. Trepanning drilling can be realized either by using 2-D scanner with F-theta lens or by using translational stages with focal lens. A number of passes were required for the complete drilling of the glass material, and good quality of micro-hole array pattern was obtained.

Figure 3 shows the SEM view of the drilled hole in soda lime glass drilled using motion stage and microscope objective. The laser parameters used include 26.0 J/cm^2 fluence, 105 kHz repetition rate, and 1 mm/s trepanning speed. The hole has the entrance and exit diameters of 400 and 230 μm, respectively. The thickness of the glass is 1 mm. A higher-magnification SEM view shows the sidewalls of the drilled hole in Fig. 3(b). The inner wall surface is irregular due to the brittle structure of glass. The drilled holes have good circular geometry for both entrance and exit sides and no micro-crack or thermal damage is observed around the edges, which is better than the results using long-pulsed lasers.

For holes drilled by using ns and ps lasers by other researchers, cracks are clearly seen around the exit side of the ns laser drilled hole, and thermal damage is visible for both ns and ps laser drilled holes.[17,18] The difference is mainly due to the fact that the fs laser pulse length is ultrashort compared to the timescale for thermal diffusion into the material. The buildup of thermal and mechanical stresses in the material is largely suppressed. The ability to drill such holes and hole arrays with consistent regular shape using fs laser is promising and remarkable due to the deterministic nature of fs laser material interaction. Even more exciting is the fact that no postprocessing is required. Further improvement of the taper angle and aspect ratio can be achieved by using scanner with F-theta lens or liquid-assisted rear side drilling.[1,3,7] It should be pointed out that thermal damage and cracking can be pronounced even for fs laser when the laser fluence and the repetition rate are set too high to increase the drilling efficiency.[19,20]

However, trepanning drilling using motion stage is slow and has low throughput for industrial applications. Trepanning drilling using scanner can increase the speed. Figure 4 shows the entrance side view of soda lime glass drilling results using scanner. The drilling is conducted by using different trepanning speeds and repeat times as shown in this figure. The other laser parameters used include 20.4 J/cm^2 fluence, 100 kHz repetition rate, and 100 mm focal length. The hole diameter is about 60 μm. As shown in Fig. 4, for lower trepanning speed, although only 10 repeat times are needed to drill through, the crack and collateral damage are severe due to the large pulse overlapping; for higher trepanning speed, although the number of repeat times is increased (e.g., 200 repeat times for 100 mm/speed), the crack and collateral damage are greatly reduced or even invisible. For speed >200 mm/s, the roundness of the hole becomes worse, possibly due to the dithering of the scanner at this high scan speed.

Figure 5 shows the SEM view of the drilled hole in stainless steel using microscope objective. The laser parameters used include 30.6 J/cm^2 fluence, 225 kHz repetition rate, and 1 mm/s trepanning speed. The hole drilled has the entrance and exit diameters of 400 and 300 μm, respectively. The total thickness of the sample is 200 μm. Figure 5(b) shows the higher magnification SEM view of the sidewalls

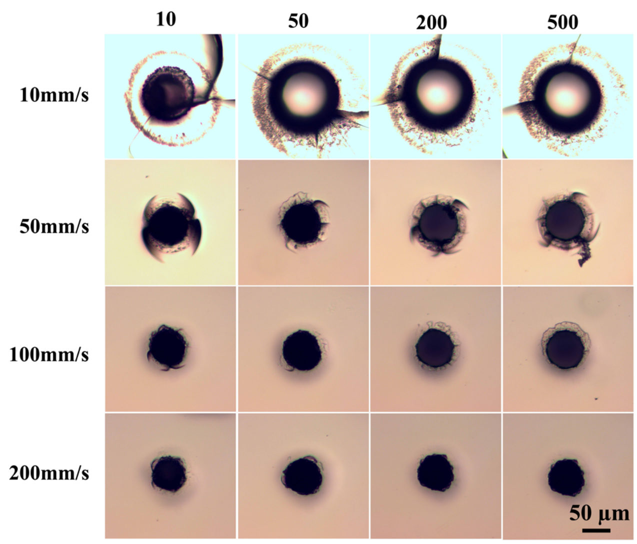

Fig. 4 Microscope view of glass drilling using scanner with different speeds and repeat times.

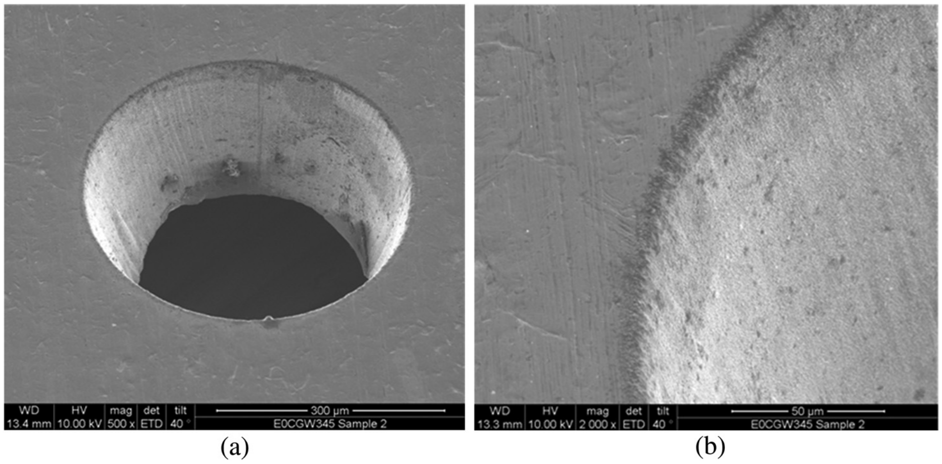

Fig. 5 SEM view of the drilled hole in stainless steel using fs fiber laser: (a) Overview and (b) detail view of hole sidewall.

of the drilled hole. The drilled holes have good circular geometry for both entrance and exit sides. It can be seen that the machined hole walls have good surface roughness of micron size and no visible micro-cracks are present around the edges. Comparing with the results using ns or ps lasers, there is a large amount of melt droplets redeposited on the hole edge[21] and a heat-affected zone is observed around the hole edge affecting the sharpness and quality of the hole.[22] The comparison with ns and ps laser drilling results clearly shows the advantage of fs laser drilling.

Furthermore, deeper hole drilling was investigated using fs fiber laser and scanner. Figure 6 shows the top and side view of a deeper hole drilled on another stainless steel sample. The stainless steel sample has a thickness of 813 μm. The roundness of the hole on the entrance side and exit side was quite good. The diameter of the hole entrance is 290 μm and that of the exit is 150 μm. The taper angle is <5 deg. The maximum aspect ratio achieved in this study is 8∶1 with hole entrance diameter of 100 μm and taper angle around 2 deg.

Figure 7(a) shows the stainless steel drilling depths as a function of repeat times using scanner. The repetition rate is 225 kHz and the fluence used is 2.0 J/cm^2. For 5 mm/s scan speed, at the beginning, the drilling depth grows fast (5 to 10 μm/scan for 5 mm/s) with the repeated trepanning time. When it reaches around 100 μm, it grows slow (<1 μm/scan) with the repeat times; it becomes even slower when it goes to 200 μm deep. For 1 mm/s scan speed, the drilling depth is >5 mm/s for the same repeat times, but it also goes slow when it reaches above 100 μm and the difference between the two speeds becomes smaller when the repeat time is >100.

Possible explanations include that the laser beam energy is attenuated due to block and scattering, and the ablated material is harder to get out as the beam is focused deeper. Figure 7(b) shows the bottom surface of partially drilled hole in stainless steel. Interestingly, fine subwavelength ripple structure is observed with about 170 nm width and 5 to 10 μm length. The ripple spacing is generally <100 nm, and some of the ripples are close to each other without spacing. The orientations of the ripple structures are parallel to each other. It is not clear whether or not the generation of these ripples is caused by interference effects and their orientations depend on laser polarization. Further investigation is needed. Similar ripple structure has been observed in various materials for fs laser drilling.[13,14] Smooth surfaces are generally preferred for precision machining and micro-fluidics, whereas rippled structures can find applications in grating fabrication and adhesion of deposited materials.

Since the first use of lasers in the medical field, medical applications such as diagnosis and tissue processing have been in the focus of interest to replace conventional surgical

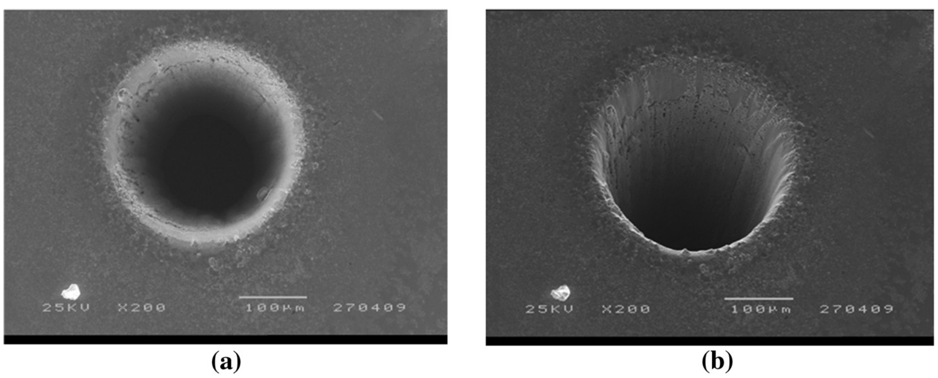

Fig. 6 SEM view of deep hole drilling in stainless steel using fs fiber laser: (a) Top view and (b) side view of hole sidewall.

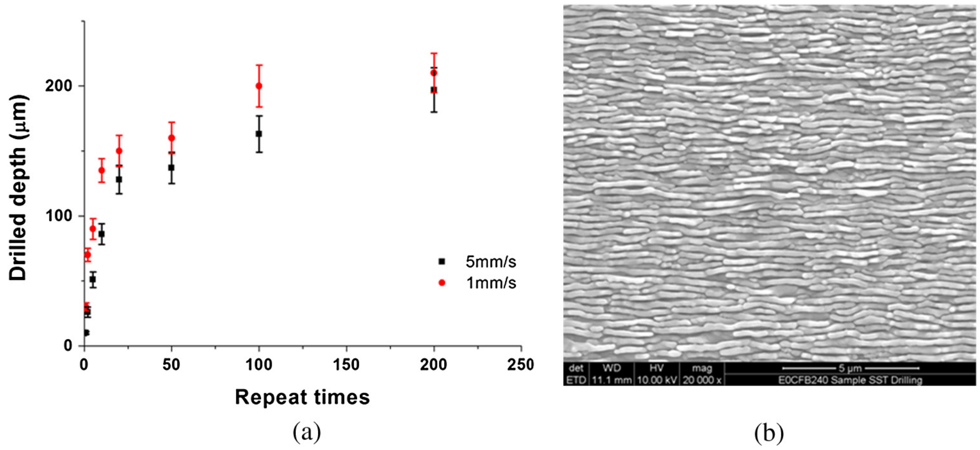

Fig. 7 (a) Stainless steel drilling depths as function of repeat time using scanner. (b) SEM view of ripple structure on bottom of the drilled hole in stainless steel using fs fiber laser.

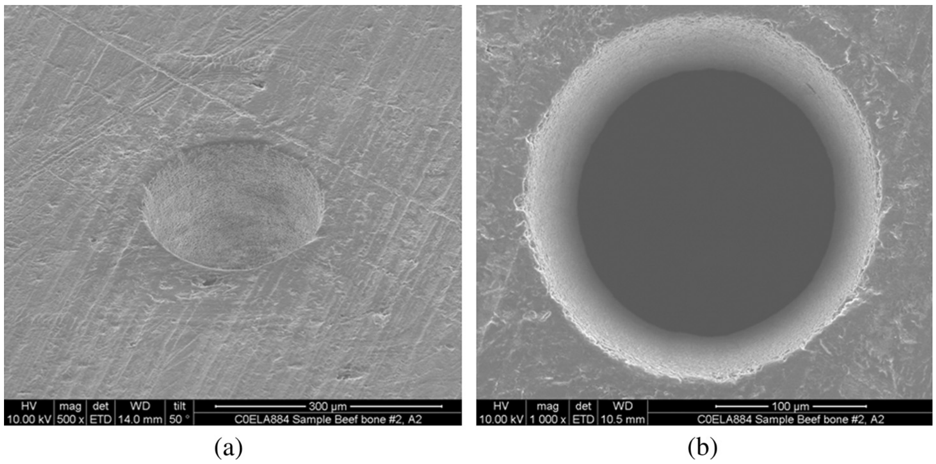

Fig. 8 Micro-hole drilling in bovine bone using fs fiber laser: (a) SEM overview and (b) SEM top view.

tools. Conventional long-pulsed lasers have not succeeded in replacing the bone drill in many hard tissue applications, mainly due to the unacceptable collateral damage. In this study, tissue hole drilling was demonstrated using fs fiber laser, as shown in Figs. 8 and 9. Figure 8(a) shows the SEM overview of the hole drilling results in bovine bone and Fig. 8(b) shows the SEM top view. The laser parameters used include 12.0 J/cm^2 fluence, 50 kHz repetition rate, and 1 mm/s trepanning speed. The depth of bovine bone is about 300 μm. The drilled hole has entrance diameter of 230 μm and exit diameter of 173 μm. The drilled holes have good circular geometry for both entrance and exit sides, and no thermal damage is observed around the edges.

Figure 9 shows the microscope view of the hole drilling results in soft tissue (bovine tendon) using fs fiber laser. It was processed using 12.0 J/cm^2 fluence, 50 kHz repetition rate, and 1 mm/s trepanning speed. The drilled hole has a diameter of 400 μm and a depth of around 500 μm. There is a minimal heat-affected zone near the edge due to the repeated trepanning times.

The energy absorption process has been studied in the context of fs laser ablation.[9–11,14,16,23] It takes place following

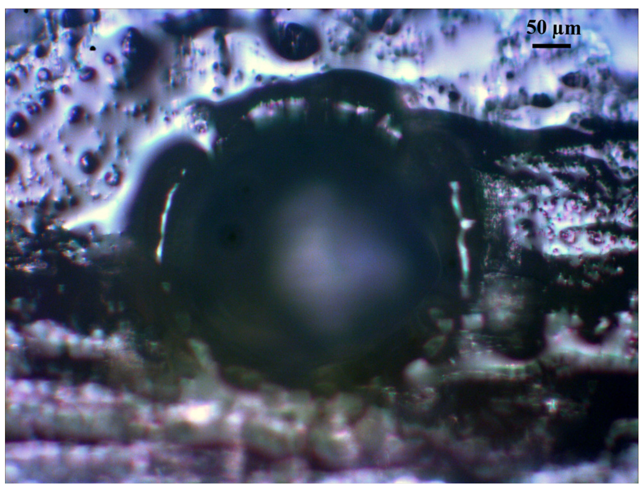

Fig. 9 Microscope view of micro-hole drilling in bovine tendon using fs fiber laser.

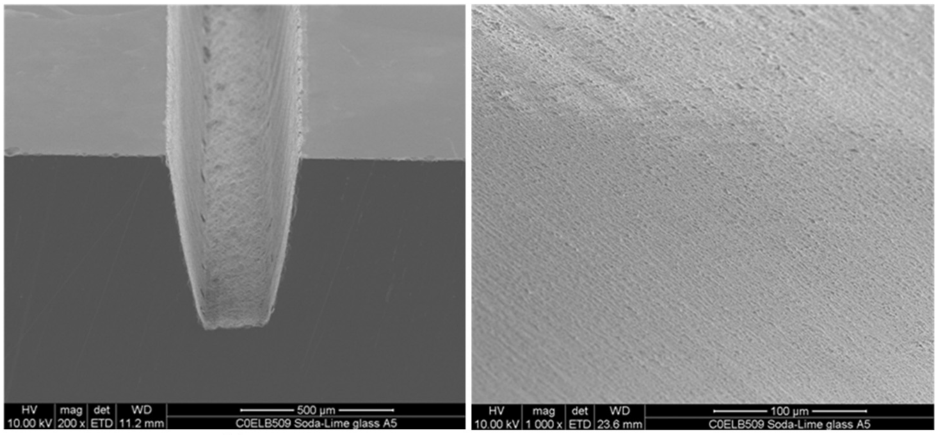

(a) (b)

Fig. 10 (a) SEM cross section view of soda lime glass trench written by using fs fiber laser and (b) SEM detail view of sidewall.

the sequential steps—production of initial seed electrons, avalanche photoionization, and plasma formation. The laser energy is only absorbed in the small focal volume of the laser, where the intensity is high enough for multiphoton ionization to occur in less than ps. The energy dissipation process involves the transfer of the energy from the hot plasma created by laser pulses to the lattice, resulting in the modified regions in the material. This process is less well understood than the energy absorption process. It is known that the dissipation process occurs on a timescale of hundreds of ns to μs; this is substantially longer than the hundreds of fs required for the energy absorption process. It is believed that the primary dissipation mechanisms are a combination of thermal diffusion and shockwave generation, though it remains uncertain which process is dominant. This may depend on the precise writing conditions (pulse fluence, repetition rate). The end results of the fs laser-material interaction are related with physical, chemical, and mechanical changes of the material after exposure to the laser beam. A rule of thumb is that when the pulse width is <1 ps, the thermal diffusion can be confined in micron dimension and HAZ can be eliminated.

As shown in Figs. 8 and 9, the remarkable finding is the complete absence of visible cracks or thermal damage around the edges of the drilled holes. This is totally different from the results using CW or long-pulsed lasers. Typically, treatment by a conventional pulsed laser (ns-to-ms pulse width) leads to cracking, melting, charring of the surrounding materials from a few tens of microns to a few hundreds of microns range.[24,25] The use of fs fiber laser would allow the implementation of cheaper, compact, and reliable laser systems for life science and medical applications.

Furthermore, trench micromachining and cutting were also studied for different materials. Figure 10 gives an example of soda lime glass trench micromachining using fs fiber laser. As shown in this figure, the trench width is 400 μm and depth is about 760 μm. The laser parameters used include 100 kHz repetition rate and 10.0 J/cm^2 fluence. The scanning speed is 200 mm/s, and multiple lines with space between lines were used in the trench writing. It can be seen from the cross-section view that sidewalls are almost vertical and the angles on both sides are around 85 deg near the opening of the trench; when the trench goes deeper, the sidewall angles decrease and the trench becomes a "U" shape. This is a typical shape for Gaussian beam; when the trench goes deeper, the ablated materials and debris are harder to get out; the laser beam energy is attenuated due to large focus angle and scattering of ablated debris and

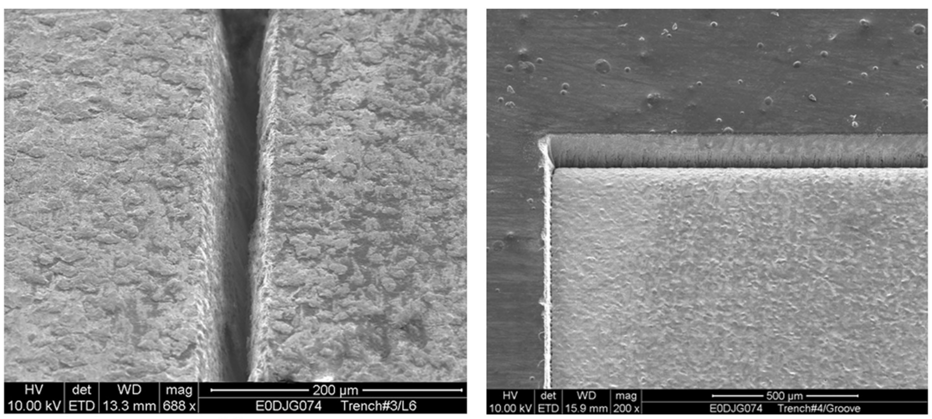

(a) (b)

Fig. 11 SEM view of titanium trench and micro-cavity micromachining by using fs fiber laser. (a) Trench micromachining and (b) micro-cavity micromachining.

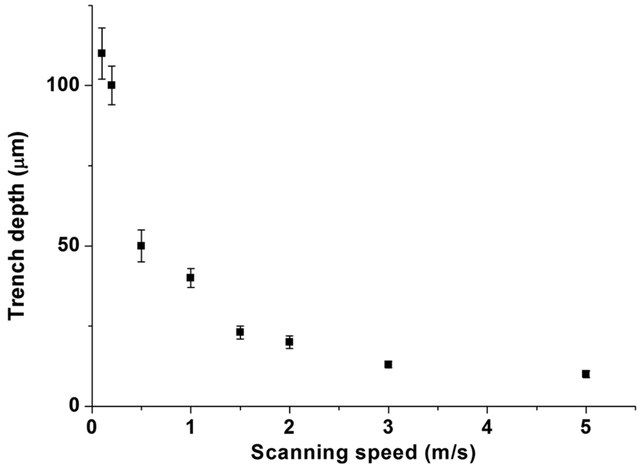

Fig. 12 Titanium trench depth written using fs fiber laser for different speeds.

sidewall. Figure 10(b) shows the SEM detailed view of the sidewall and the roughness on both sides is on the order of μm.

Figure 11(a) shows another example of titanium trench micromachining using fs fiber laser. The trench width is 50 μm and depth is about 100 μm. The laser parameters used include 100 kHz repetition rate and 1.0 $\mathrm{J/cm^2}$ fluence. The scanning speed is 200 mm/s, and multiple lines with space between lines were used in the trench writing. Totally 800 passes were used to achieve this depth. The focus position was properly adjusted when the micromachining went deeper. Figure 11(b) shows the micro-cavity and trench micromachining using fs fiber laser with the same laser parameters. The rectangular micro-cavity has a depth of 100 μm. A deeper trench is written at the top of the micro-cavity with 50-μm wide and 200-μm deep.

Furthermore, different writing speeds were used to study the effect on titanium trench writing depth. The trench width is 50 μm, the scanning repeat time is fixed at 200, and the scanning speed is from 0.1 to 5 m/s. The laser parameters used are same as Fig. 11. Figure 12 shows the measured trench depth written using fs fiber laser for different speeds. Higher pulse energy and faster scanning speed can greatly enhance the writing efficiency; for example, it needs only 200 repeated times to write 100 μm deep with 5.3 $\mathrm{J/cm^2}$ fluence compared with 800 times for 1.0 $\mathrm{J/cm^2}$ fluence shown in Fig. 10(a). In addition, for the same fluence, higher scan speed gives lower efficiency since the ablation threshold is higher due to less pulse overlap and incubation effect.

4 Summary

In this paper, micro-hole drilling and cutting of different materials using an fs fiber laser were investigated. The quality of drilled holes for different materials was characterized using optical microscope and SEM. Debris-free micro-holes with sharp edge and no thermal damage were achieved for both glass and metal with the aspect ratio of 8:1. Furthermore, the absence of visible cracks and thermal damage was observed around the edges of the drilled holes in both hard and soft tissues. Trench micromachining and cutting were also studied for different materials. Glass and metal trench micromachining examples were shown with straight clean edges and thermal damage is invisible. This fs fiber laser direct writing technique can be applied in the fabrication of microfluidic devices, biomedical devices, photonic devices, lab-on-chip devices, sensors, and micro-optics.

Acknowledgments

This work was funded by NSF and AFOSR.

References

1. D. Hwang, T. Choi, and C. Grigoropoulos, "Liquid-assisted femtosecond laser drilling of straight and three-dimensional microchannels in glass," *Appl. Phys. A: Mater. Sci. Process.* **79**(3), 605–612 (2004).
2. Y. Matsuoka, Y. Kizuka, and T. Inoue, "The characteristics of laser micro drilling using a Bessel beam," *Appl. Phys. A: Mater. Sci. Process.* **84**(4), 423–430 (2006).
3. R. An et al., "Simultaneous multi-microhole drilling of soda-lime glass by water-assisted ablation with femtosecond laser pulses," *Opt. Express* **13**(6), 1855–1859 (2005).
4. Y. Bellouard et al., "Fabrication of high-aspect ratio, micro-fluidic channels and tunnels using femtosecond laser pulses and chemical etching," *Opt. Express* **12**(10), 2120–2129 (2004).
5. A. Marcinkevičius et al., "Femtosecond laser-assisted three-dimensional microfabrication in silica," *Opt. Lett.* **26**(5), 277–279 (2001).
6. M. Bhuyan et al., "High aspect ratio taper-free microchannel fabrication using femtosecond Bessel beams," *Opt. Express* **18**(2), 566–574 (2010).
7. X. Zhao and Y. C. Shin, "Femtosecond laser drilling of high-aspect ratio microchannels in glass," *Appl. Phys. A: Mater. Sci. Process.* **104**(2), 713–719 (2011).
8. S. Darvishi, T. Cubaud, and J. P. Longtin, "Ultrafast laser machining of tapered microchannels in glass and PDMS," *Opt. Lasers Eng.* **50**(2), 210–214 (2011).
9. S. Nikumb et al., "Precision glass machining, drilling and profile cutting by short pulse lasers," *Thin Solid Films* **477**(1–2), 216–221 (2005).
10. S. Juodkazis et al., "Hole drilling in stainless steel and silicon by femtosecond pulses at low pressure," *Appl. Phys. A: Mater. Sci. Process.* **79**(4–6), 1555–1559 (2004).
11. G. Kamlage et al., "Deep drilling of metals by femtosecond laser pulses," *Appl. Phys. A: Mater. Sci. Process.* **77**(2), 307–310 (2003).
12. A. Ancona et al., "Femtosecond and picosecond laser drilling of metals at high repetition rates and average powers," *Opt. Lett.* **34**(21), 3304–3306 (2009).
13. A. Weck et al., "Ripple formation during deep hole drilling in copper with ultrashort laser pulses," *Appl. Phys. A: Mater. Sci. Process.* **89**(4), 1001–1003 (2007).
14. A. Weck et al., "Laser drilling of high aspect ratio holes in copper with femtosecond, picosecond and nanosecond pulses," *Appl. Phys. A: Mater. Sci. Process.* **90**(3), 537–543 (2008).
15. G. Mak, E. Lam, and H. Choi, "Precision laser micromachining of trenches in GaN on sapphire," *J. Vac. Sci. Technol., B: Microelectron. Nanometer Struct.* **28**(2), 380–385 (2010).
16. S. Baudach, J. Bonse, and W. Kautek, "Ablation experiments on polyimide with femtosecond laser pulses," *Appl. Phys. A* **69**(1), S395–S398 (1999).
17. B. Keiper et al., "Drilling of glass by excimer laser mask projection technique," *J. Laser Appl.* **12**, 189–193 (2000).
18. S. Lee, A. Ashmead, and L. Migliore, "Comparison of ns and ps pulses for Si and glass micromachining applications," *Proc. SPIE* **7193**, 719322 (2009).
19. H. Varel et al., "Micromachining of quartz with ultrashort laser pulses," *Appl. Phys. A: Mater. Sci. Process.* **65**(4–5), 367–373 (1997).
20. J. Kaspar et al., "Laser helical drilling of silicon wafers with ns to fs pulses: scanning electron microscopy and transmission electron microscopy characterization of drilled through-holes," *J. Laser Appl.* **18**, 85 (2006).
21. R. Witte et al., "Laser micro-drilling with nanoseconds: parametrical influences and results," *Proc. SPIE* **7022**, 702208 (2007).
22. F. Dausinger, H. Hugel, and V. I. Konov, "Micromachining with ultrashort laser pulses: from basic understanding to technical applications," *Proc. SPIE* **5147**, 106–115 (2002).
23. M. Obara et al., "Femtosecond laser processing tailored for biomedical materials and laser power delivery through optical fibers," in *High-Power Lasers and Applications*, International Society for Optics and Photonics, pp. 123–135 (2003).
24. K. M. Sasaki et al., "Ultrastructural analysis of bone tissue irradiated by Er: YAG laser," *Lasers Surg. Med.* **31**(5), 322–332 (2002).
25. T. J. Flotte, R. Anderson, and T. F. Deutsch, "Pulsed CO2 laser tissue ablation: effect of tissue type and pulse duration on thermal damage," *Lasers Surg. Med.* **8**(2), 108–118 (2005).

Huan Huang is currently a project manager at PolarOnyx, Inc. He received his PhD from Rutgers University, New Brunswick, in 2010. His research interests include biomedical and micro/nano-scale applications of ultrashort pulsed lasers, especially in laser-tissue interaction, laser micro/nano-fabrication, laser micro-processing of tissue, nonlinear imaging, and laser induced breakdown spectroscopy.

Lih-Mei Yang received the PhD from University of Michigan, Ann Arbor, in 1996 and demonstrated the first high-energy femtosecond up-conversion fiber laser using multimode gain fiber. In 2000, she joined the amplifier team of the Lucent Technologies, Microelectronics Group, and led to design fiber amplifiers including Raman amplifiers. In 2005, she joined PolarOnyx to develop all fiber-based femtosecond fiber lasers and is a key member for the development of high energy/power femtosecond fiber lasers.

Jian Liu is the founder of PolarOnyx, Inc. He earned his PhD from the University of Texas at Austin. He led Lucent/Bell Labs L-band erbium-doped fiber (EDF) development. In PolarOnyx, he led the development of a series of award-winning femtosecond fiber laser products. He has authored over 60 publications and over 28 patents. He is a member of SPIE and OSA.